Polymers **2013**, *5*, 45-55; doi:10.3390/polym5010045

OPEN ACCESS

polymers

ISSN 2073-4360

www.mdpi.com/journal/polymers

Article

Fabrication of Pd Doped WO_3 Nanofiber as Hydrogen Sensor

Alireza Nikfarjam [1], Somayeh Fardindoost [2] and Azam Iraji zad [2,3,*]

[1] Faculty of New Sciences & Technologies, University of Tehran, P.O. Box 14395-1374, Tehran, Iran; E-Mail: a.nikfarjam@ut.ac.ir

[2] Department of Physics, Sharif University of Technology, Azadi Street, P.O. Box 11365-9161, Tehran, Iran; E-Mail: fardindoost@mehr.sharif.edu

[3] Institute for Nanoscience and Nanotechnology, Sharif University of Technology, Azadi Street, P.O. Box 11155-8639, Tehran, Iran

***** Author to whom correspondence should be addressed; E-Mail: iraji@sharif.edu; Tel.: +98-21-6616-4513; fax: +98-21-6600-5410.

Received: 18 November 2012; in revised form: 10 December 2012 / Accepted: 25 December 2012 / Published: 10 January 2013

Abstract: Pd doped WO_3 fibers were synthesized by electro-spinning. The sol gel method was employed to prepare peroxopolytungstic acid (P-PTA). Palladium chloride and Polyvinyl pyrrolidone (PVP) was dissolved in the sol Pd:WO_3 = 10% molar ratio. The prepared sol was loaded into a syringe connected to a high voltage of 18.3 kV and electrospun fibers were collected on the alumina substrates. Scanning electron microscope (SEM), X-ray powder diffraction (XRD) and X-ray photoelectron spectroscopy (XPS) techniques were used to analyze the crystal structure and chemical composition of the fibers after heat treatment at 500 °C. Resistance-sensing measurements exhibited a sensitivity of about 30 at 500 ppm hydrogen in air, and the response and recovery times were about 20 and 30 s, respectively, at 300 °C. Hydrogen gas sensing mechanism of the sensor was also studied.

Keywords: Pd doped WO_3 nanofiber; hydrogen sensor; electrospinning; sensing mechanism

---

1. Introduction

Hydrogen burns cleanly without releasing pollutants or greenhouse gases and therefore, in recent years, more attention has been paid to hydrogen as an excellent candidate for fossil fuel replacement in

household and transportation applications. However, hydrogen is a highly flammable fuel with a wide combustion range of 4%–75%. Besides, it has a large diffusion coefficient of 0.61 cm^2/s in air. Therefore, detection and leakage control of this gas is a challenging subject. Today, development of a hydrogen sensor with negligible power consumption and high stability, sensitivity and fast response is desired.

Reports of various technologies for hydrogen sensing include FETs [1,2], optical fibers [3,4], thermoelectric [5,6], Schottky diodes [7–9], surface acoustic wave devices [10,11] and metal oxides [12–17]. Metal oxide sensors are under intensive development and have been studied for decades [18,19]. In metal oxide sensors, the electrical resistance of the film changes when exposed to a target gas. Also, among metal oxides, WO_3 is widely used to detect many gases like H_2, H_2S, NO_2 and VOC [20–23]. Moreover, it has been shown that the addition of an appropriate amount of noble metal additives promotes chemical reactions by reducing activation energy between the surface of metal oxide and target gas. Also, this increases the response and selectivity as well as decreasing the maximum working temperature of the sensors. For hydrogen sensors, modification of metal oxides, especially WO_3, by metal additives such as Pt, Pd, or Au, using different techniques is under intensive investigation [24–31].

It is known that gas absorption depends on the surface area, which is affected by the preparation method. Increasing the surface to volume ratio to enhance gas sensing properties is currently under development by introducing different nanostructures such as nanowires, nanorods, nanobelts and nanofibers. Nanofibers have high density of surface sites that make them excellent candidates for gas sensing applications [32].

Among different fabrication methods, electrospinning is a simple and cost effective method for preparing one dimensional materials. Recently, several researches have reported fabrication of metal oxide nanofibers [33–39] in which metal oxide nanoparticles can be added to a polymer matrix to make nanocomposite fibers. Heat treatment removes polymer and leaves metal oxide material with fiber shape.

Metal oxide fibers could be synthesized by combining sol-gel and electrospinning methods. Adding catalysts to the solution (sol) produces nanofibers with improved catalytic properties for selective gas detection at lower temperatures. Polymer matrix can be decomposed through heat treatment and leaves metal oxide fiber with lengths from several hundred nanometers to few micrometers.

Preparing one dimensional WO_3 fibers by sol-gel method was first reported by Lu *et al.* [40]. Others used pure WO_3 fiber for detecting ammonia, NO_2 and CO gasses [41,42]. In our previous work [29], the sensitivity of both pure and Pd-modified WO_3 thin films was measured towards hydrogen as a function of operating temperatures in the range of 30 °C to 350 °C. A systematic increase in sensitivity was observed for the modified films in the whole temperature range. The sensitivity increased due to a reduction of the activation energy between the WO_3 surface and the hydrogen gas in the presence of Pd (PdO). It was seen that the sensitivity of Pd:W = 10% films have considerable amounts at room temperature and the working temperature (the temperature which has maximum sensitivity) decreased by increasing the Pd concentrations.

Since high response and recovery times were observed at low working temperatures. Given the results of our previous experiments on Pd modified WO_3 films, we decided to study structure effect on modification of sensing behavior. Therefore, a combination of electrospinning and the sol gel method

was studied to compare the result of the sensing behavior of Pd:WO_3 thin film with the electrospun Pd doped WO_3 nanofiber samples with the same ratio (Pd:W = 10%). In this work, we prepared WO_3 nanoparticles by the sol-gel method and then Pd and PVP were added to the sol. To remove polymer and make WO_3 nanoparticles with fiber shape, samples were annealed in air at 500 °C for 1 h. The Pd doped WO_3 nanofibers showed fast response time and high sensitivity toward hydrogen gas at low temperature.

2. Experimental Section

In our sol-gel route, Peroxopolytungstic acid (P-PTA) sol was prepared according to the Kudo route [43]. Five grams of tungsten wire and 20 mL of H_2O_2 (30%) was stirred at room temperature for 48 h until the whole tungsten wire was dissolved. Unreacted H_2O_2 was removed by using platinum net. Then 20 mL ethanol was added and the solution was heated at 80 °C which resulted in a sol color change from clear to orange.

For the activation process we used Pd catalyst. Since in our previous report, we obtained best sensitivity for Pd:W = 10% molar ratio [29], we chose this ratio for adding $PdCl_2$ salt (Merk) directly to the P-PTA sol.

To fabricate fibers, 1.0 g polyvinyl pyrrolidone (PVP) (Aldrich) was added into the P-PTA sol and was stirred for one day. The resulting solution was loaded into a plastic syringe and its needle was connected to a high-voltage DC supply up to 30 kV. A voltage of 18.3 kV was applied between the needle and grounded target. Al_2O_3 substrates were placed on a piece of flat aluminum with 20 cm distance from the tip of the needle to collect fibers. The prepared samples were annealed in air at 500 °C for 1 h.

X-ray powder diffraction (XRD) analysis was recorded by a Philips X'pert instrument operating with CuKα radiation (λ = 1.54178 Å) at 40 kV/40 mA. A Philips XL30 model Scanning electron microscope (SEM) was used to obtain the SEM images. For the X-ray photoelectron spectroscopy (XPS) experiment, an Al anode X-ray source was employed with a concentric hemispherical analyzer (Specs model EA10 plus) to analyze the energy of the emitted photoelectrons. Gas sensing properties of the as-fabricated sensor were measured using a static test system. A data logger was used to collect the data and the whole system was automatically controlled by computer.

For measuring the electrical resistance, Au/Ti comb-like interdigitated electrodes with 150 nm thickness were evaporated on the sample surface through a mask. The samples were placed in a small stainless steel chamber with several electrical feed-through, gas inlet and gas outlet. For measuring sensitivity, a constant dc voltage of 5 V was applied to the circuit; including the sensor in series with a constant resistor. Voltage variation across the resistor was measured. During the measurements, the fibers were warmed by a heater located on the back of the substrates. We used dry air as the reference gas and hydrogen as the target gas. Sensitivity was defined as $S = (Vrg - Vra)/Vra$, where *Vrg* and *Vra* are the sensor voltage in the presence and absence of hydrogen, respectively. The measurement setup consists of mass flow controllers and a data acquisition system for recording resistance changes. We define the response time as the time taken for the sensor's resistance to undergo a 90% variation with respect to its equilibrium value and recovery time as the time taken to achieve 60% variation to reach

its initial value in air after the removal of H_2. The gas sensing performance was tested at hydrogen concentration of 500 ppm in the range of 30 °C to 300 °C.

3. Results and Discussion

3.1. Structure Analysis

SEM images of as-spun PVP composite fibers and the sintered fibers at 500 °C for 1 h are displayed in Figure 1a,b, respectively. Figure 1a shows the used Aluminum foil surface and some PVP composite fibers with an average diameter of about 500 nm. The heating process compresses the fibers and reduces their average thickness to about 150 nm while keeping their morphology as is shown in Figure 1b. Heat treatment at 500 °C removes the polymer and leaves metal oxide material with fiber shapes. SEM images show continuous fibers with lengths of several tens micrometers. By electrospinning, a huge number of fibers electrospun over the substrate and form as a film. To observe better by SEM, we made a sample with low density fibers (Figure 1a,b). Figure 1c shows another sample with high density of fibers (sample for gas sensing experiments). Both high fibrous surface area as well as high porosity increase effective sensitive surface area.

Figure 1. Scanning electron microscope (SEM) images of (**a**) as spun Polyvinyl pyrrolidone (PVP)/Pd/ peroxopolytungstic acid (P-PTA) fiber; (**b**) WO_3 fiber, after sintering at 500 °C for 1 h; (**c**) sintered sample with high density of fibers.

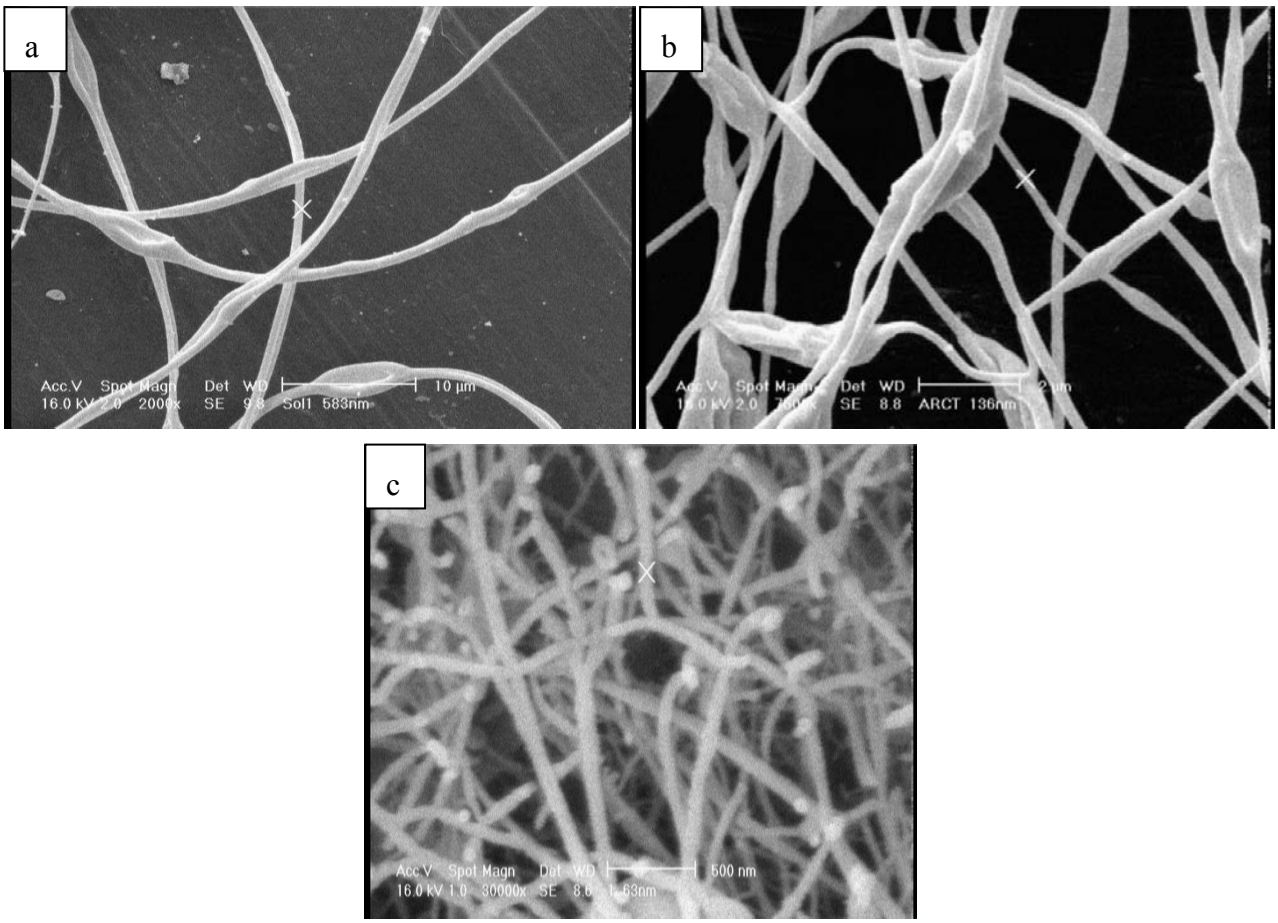

As presented in Figure 2, heat treatment at 500 °C resulted in the formation of crystals of both monoclinic WO_3 and oxidized Pd. The evidence of PdO after annealing can be observed by XPS analysis. Data in Figure 3a indicates that the surface of the annealed Pd doped WO_3 nanofiber is composed of tungsten, oxygen, carbon contamination, and small amounts of palladium. Figure 3b, shows the peaks related to palladium oxide formation after the annealing process.

Figure 2. The X-ray powder diffraction (XRD) pattern of the Pd doped WO_3 nanofiber sintered at 500 °C.

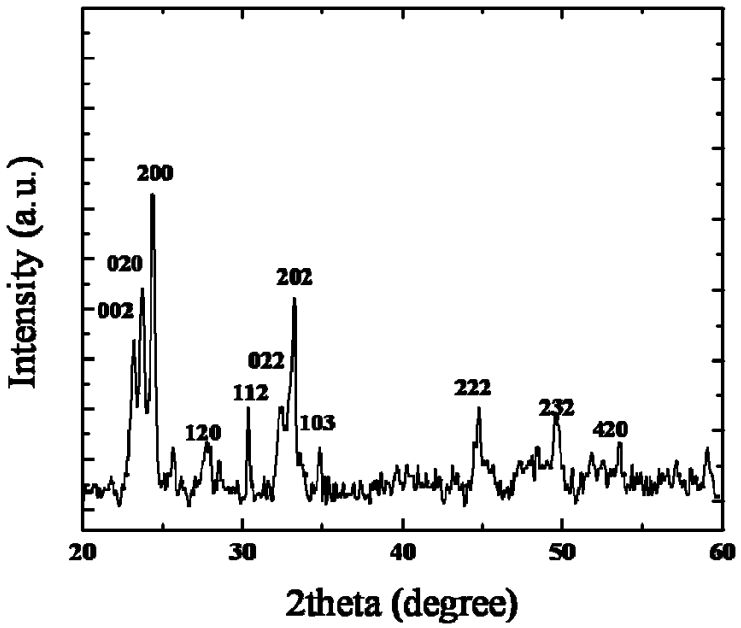

Figure 3. The X-ray photoelectron spectroscopy (XPS) patterns of the Pd doped WO_3 nanofiber that was heat treated at 500 °C, (**a**) Peak survey and (**b**) Deconvolution in the Pd 3d region.

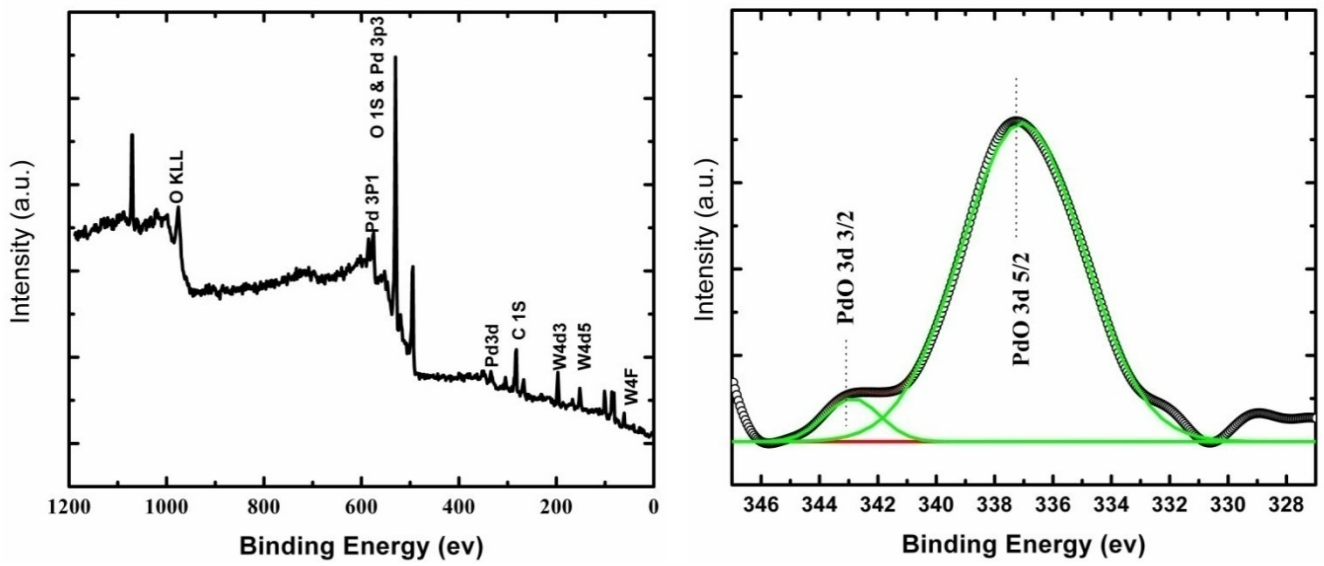

3.2. Hydrogen Sensing Measurements

Hydrogen sensing properties of the Pd-modified WO_3 samples were investigated while they were exposed to 500 ppm H_2 at different operating temperatures. Figure 4 shows the changes in the voltage of a series resistor *vs.* time (transient response). The used electrical circuit is shown in the inset of Figure 4. It presents fast response and recovery times of about 20 and 30 s, respectively.

Figure 4. Normalized voltage variation across the series resistor as output signal

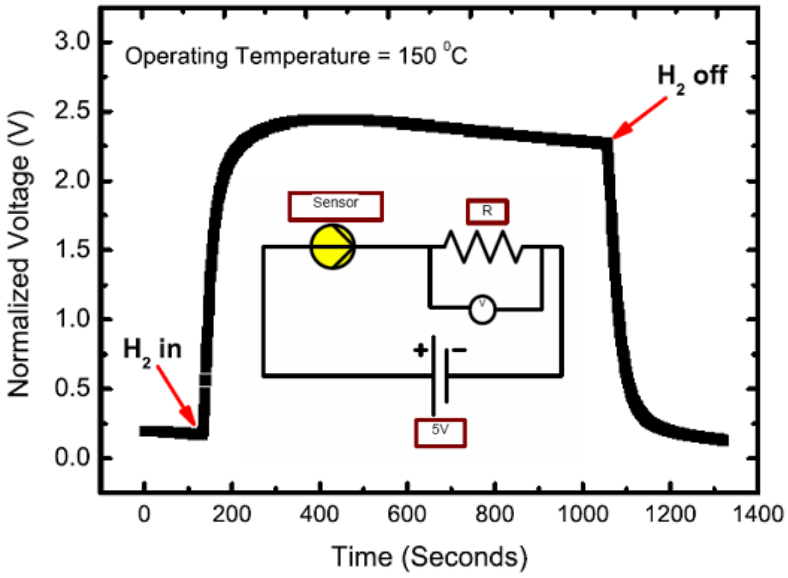

We measured the sensitivity of the samples as a function of operating temperature in the range of 75 °C to 300 °C. As shown in Figure 5, the sensitivity is noticeable at a temperature of about 75 °C and it is enhanced by increasing the operating temperature to 300 °C. This high sensitivity may be attributed to the reduction of the activation energy between the WO_3 surface and hydrogen gas in the presence of Pd (PdO).

Figure 5. The sensitivity of the Pd-modified WO_3 nanofiber towards 500 ppm hydrogen as a function of operating temperature.

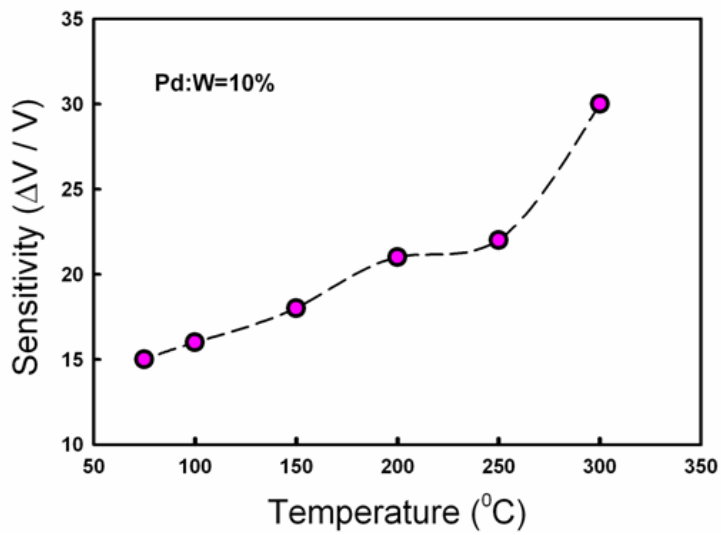

Response and recovery times of the Pd-modified WO_3 fiber for 500 ppm hydrogen are presented in Figure 6. It presents a decaying behavior with considerable fast response and recovery times at high temperatures (300 °C). At low working temperature the response time is higher due to slow desorption of the formed water molecules on the surface especially at temperatures below 100 °C.

Figure 6. The response and recovery times of the Pd-modified WO_3 nanofiber towards 500 ppm hydrogen as a function of operating temperature.

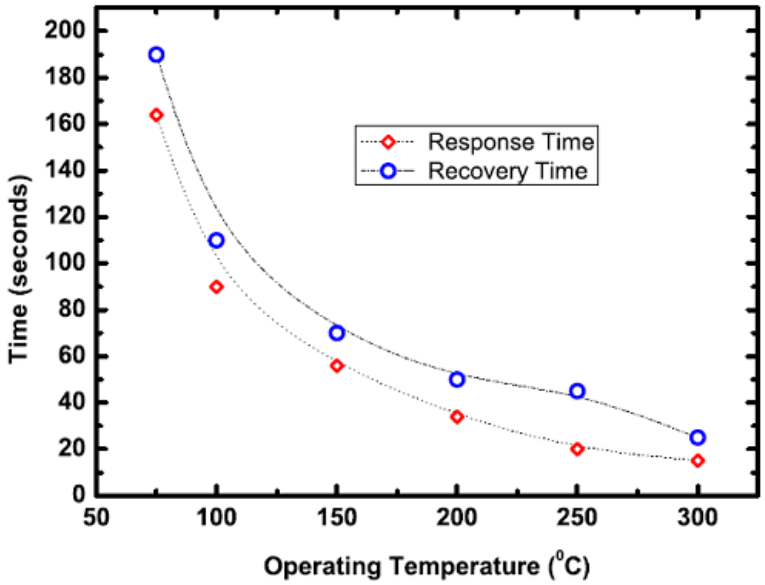

Our results demonstrated faster response and recovery times in the order of 160–190 s for low temperature sensing which is so considerable compare to 60 min recovery time for Pd:WO_3 = 10% in the form of thin film [29]. It can be attributed to the facilitate occupancy and desorption of H_2 molecules at grain boundaries on the large surface area of nanofibers in a porous network. However, the obtained results of the response magnitudes and the working temperature are not as good as our previous work on thin film sensors.

3.3. Hydrogen Sensing Mechanism

The WO_3 fibers have been made of small grains and grain boundary barriers are existed between neighboring grains located in a fiber structure. This structure has an increased surface area as well as providing electronic transmission channels for electron transferring between WO_3 particulates. Since WO_3 nanofibers in this study are continuous with WO_3 grains, we expect sensing mechanism of the single WO_3 fiber is principally similar to that of metal oxide films. So, grain size has important effect on sensing performances [44–46]. However, despite fibers being continuous media, there are a great number of fiber to fiber connections, where electron current passing through these connection potential barriers has an important role in total current passing through the fibers' film.

In addition, regarding our previous work [29], presence of Pd makes a systematic increase in the sensitivity in the whole temperature ranges. This can be attributed to the effect of Pd catalyst in performing electronic sensitization mechanism and reducing the activation energy between the WO_3 surface and the hydrogen gas [47]. As shown here in Figure 7a,b, the O_2 molecules chemisorb and

dissociate on the surface of the WO_3 grains. Then they trap and extract electrons from the conduction band of n-type semiconductor (WO_3) due to their high electron affinity. A depletion or space-charge region develops on the surface of the grain. This increases the potential barrier height between neighboring grains and also widens it, which is called energy band bending as shown in Figure 7a. This makes electron transferring between grains difficult which decreases the conductance of the fiber. By exposing fibers to hydrogen gas, reaction with the adsorbed oxygen molecule takes place. This re-injects captured electrons to the depletion region and the reverse effect will take place (Figure 7b).

Figure 7. Hydrogen sensing mechanism of WO_3 neighboring grains (**a**) before and (**b**) after hydrogen exposure.

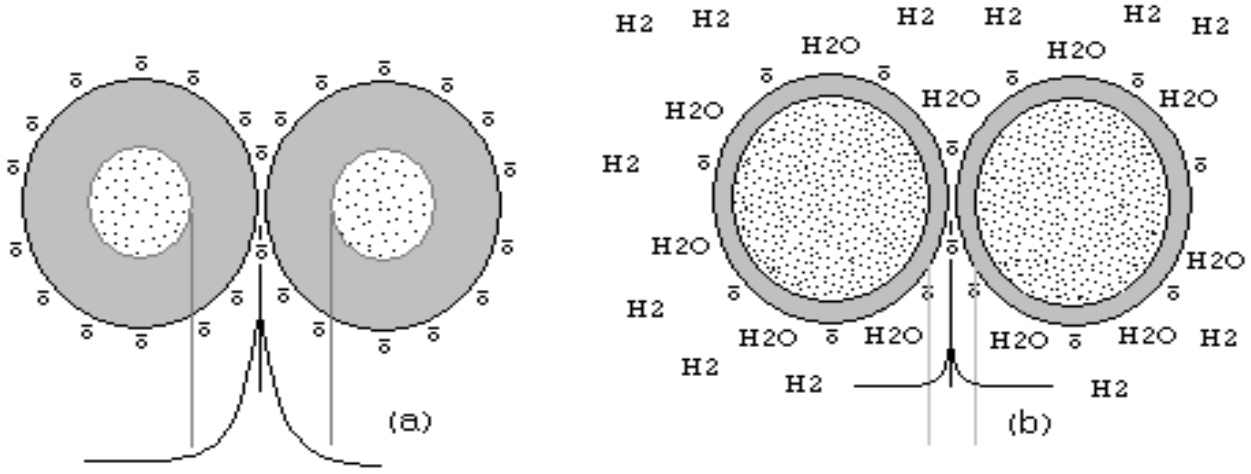

4. Conclusions

Pd doped WO_3 fibers were synthesized by combining electrospinning and sol-gel methods and were characterized by SEM, XRD and XPS methods. The sensor fabricated from these fibers exhibited high sensitivity and rapid response/recovery to hydrogen at 300 °C. The highest sensitivity was about 30 when the sensor was exposed to 500 ppm, and the response and recovery times were about 20 and 30 s, respectively. The WO_3 fiber sensors showed fast response times toward hydrogen even at low operating temperatures. These results demonstrate that Pd doped WO_3 fibers can be used as the sensing material for fabricating high performance hydrogen sensors. Besides, hydrogen gas sensing mechanism of the sensor was studied and a model proposed.

References

1. Yamaguchi, T.; Kiwa, T.; Tsukada, K.; Yokosawa, K. Oxygen interference mechanism of platinum–FET hydrogen gas sensor. *Sens. Actuators A Phys.* **2007**, *136*, 244–248.
2. Higuchi, T.; Nakagomi, S.; Kokubun, Y. Field effect hydrogen sensor device with simple structure based on GaN. *Sens. Actuators B Chem.* **2009**, *140*, 79–85.
3. Villatoro, J.; Moreno, D.L.; Monzón-Hernández, D. Optical fiber hydrogen sensor for concentrations below the lower explosive limit. *Sens. Actuators B Chem.* **2005**, *110*, 23–27.
4. Slaman, M.; Dam, B.; Schreuders, H.; Griessen, R. Optimization of Mg-based fiber optic hydrogen detectors by alloying the catalyst. *Int. J. Hydrog. Energy* **2008**, *33*, 1084–1089.

5. Nishibori, M.; Shin, W.; Izu, N.; Itoh, T.; Matsubara, I.; Yasuda, S.; Ohtani, S. Robust hydrogen detection system with a thermoelectric hydrogen sensor for hydrogen station application. *Int. J. Hydrog. Energy* **2009**, *34*, 2834–2841.
6. Huang, H.; Luan, W.; Zhang, J.S.; Qi, Y.S.; Tu, S.T. Thermoelectric hydrogen sensor working at room temperature prepared by bismuth–telluride P–N couples and Pt/g-Al_2O_3. *Sens. Actuators B Chem.* **2008**, *128*, 581–585.
7. Ito, K.; Kojima, K. Hydrogen detection by Schottky diodes. *Int. J. Hydrog. Energy* **1982**, *7*, 495–497.
8. Tang, W.M.; Lai, P.T.; Xu, J.P.; Chan, C.L. Enhanced hydrogen sensing characteristics of MI SiC Schottky-diode hydrogen sensor by trichloroethylene oxidation. *Sens. Actuators A Phys.* **2005**, *119*, 63–67.
9. Tsai, T.H.; Chen, H.I.; Lin, K.W.; Hung, C.W.; Hsu, C.H.; Chen, L.Y.; Chu, K.-Y.; Liu, W.-C. Comprehensive study on hydrogen sensing properties of a Pd–AlGaN-based Schottky diode. *Int. J. Hydrog. Energy* **2008**, *33*, 2986–2992.
10. Ippolito, S.J.; Kandasamy, S.; Kalantar-Zadeh, K.; Wlodarski, W. Layered SAW hydrogen sensor with modified tungsten trioxide selective layer. *Sens. Actuators B Chem.* **2005**, *108*, 553–557.
11. Jakubik, W.P. Investigations of thin film structures of WO_3 and WO_3 with Pd for hydrogen detection in a surface acoustic wave sensor system. *Thin Solid Films* **2007**, *515*, 8345–8350.
12. Comini, E. Metal oxide nano-crystals for gas sensing. *Anal. Chim. Acta* **2006**, *568*, 28–40.
13. Aroutiounian, V. Metal oxide hydrogen, oxygen, and carbon monoxide sensors for hydrogen setups and cells. *Int. J. Hydrog. Energy* **2007**, *32*, 1145–1158.
14. Adamyana, A.Z.; Adamyana, Z.N.; Aroutiouniana, V.M.; Arakelyana, A.H.; Touryanb, K.J.; Turner, J.A. Sol-gel derived thin film semiconductor hydrogen gas sensor. *Int. J. Hydrog. Energy* **2007**, *32*, 4101–4108.
15. Korotcenkov, G. Metal oxides for solid-state gas sensors: What determines our choice? *Mater. Sci. Eng. B* **2007**, *139*, 1–23.
16. Adamyan, A.Z.; Adamyan, Z.N.; Aroutiounian, V.M. Study of sensitivity and response kinetics changes for SnO_2 thin-film hydrogen sensors. *Int. J. Hydrog. Energy* **2009**, *34*, 8438–8443.
17. Boon-Bretta, L.; Bousek, J.; Morettoa, P. Reliability of commercially available hydrogen sensors for detection of hydrogen at critical concentrations: Part II—Selected sensor test results. *Int. J. Hydrog. Energy* **2009**, *34*, 562–571.
18. Sakai, G.; Matsunaga, N.; Shimanoe, K. Theory of gas-diffusion controlled sensitivity for thin film semiconductor gas sensor. *Sens. Actuators B Chem.* **2001**, *80*, 125–131.
19. Eranna, G.; Joshi, B.C.; Runthala, D.P.; Gupta, R.P. Oxide materials for development of integrated gas sensors—A comprehensive review. *Crit. Rev. Solid State Mater. Sci.* **2004**, *29*, 111–188.
20. Ippolito, S.J.; Kandasamy, S.; Kalantar-Zadeh, K.; Wlodarski, W. Hydrogen sensing characteristics of WO_3 thin film conductometric activated by Pt and Au catalysts. *Sens. Actuators B Chem.* **2005**, *108*, 154–158.
21. Ionescu, R.; Hoel, A.; Granqvist, C.G.; Llobet, E.; Heszler, P. Ethanol and H_2S gas detection in air and in reducing and oxidizing ambience: Application of pattern recognition to analyze the

output from temperature-modulated nanoparticulate WO_3 gas sensors. *Sens. Actuators B Chem.* **2005**, *104*, 124–131.

22. Penza, M.; Martucci, C.; Cassano, G. NO_x gas sensing characteristics of WO_3 thin films activated by noble metals (Pd, Pt, Au) layers. *Sens. Actuators B Chem.* **1998**, *50*, 52–59.
23. Luo, Sh.; Fu, G.; Chen, H. Gas-sensing properties and complex impedance analysis of Ce-added WO_3 nanoparticles to VOC gases. *Solid-State Electron.* **2007**, *51*, 913–919.
24. Veith, G.M.; Lupini, A.R. Magnetron sputtering of gold nanoparticles onto WO_3 and activated carbon. *Catal. Today* **2007**, *122*, 248–253.
25. Cabot, A.; Arbiol, J.; Morante, J.R. Analysis of the noble metal catalytic additives introduced by impregnation of as obtained SnO_2 sol-gel nanocrystals for gas sensors. *Sens. Actuators B Chem.* **2000**, *70*, 87–100.
26. Opara, U.; Ovec, K.; Orel, B.; Georg, A.; Wittwer, V. The gasochromic properties of sol-gel WO_3 films with sputtered Pt catalyst. *Pergamon* **2000**, *68*, 541–551.
27. Ruiz, A.; Arbiol, J.; Cirera, A.; Cornet, A.; Morante, J.R. Surface activation by Pt-nanoclusters on titania for gas sensing applications. *Mater. Sci. Eng. C* **2002**, *19*, 105–109.
28. Moreno, D.L.; Monzón-Hernández, D. Effect of the Pd–Au thin film thickness uniformity on the performance of an optical fiber hydrogen sensor. *Appl. Surf. Sci.* **2007**, *253*, 8615–8619.
29. Fardindoost, S.; Iraji zad, A.; Rahimi, F.; Ghasempour, R. Pd doped WO_3 films prepared by sol-gel process for hydrogen sensing. *Int. J. Hydrog. Energy* **2010**, *35*, 854–860.
30. Epifani, M.; Abriol, J.; Pellicer, E.; Comini, E.; Siciliano, P.; Faglia, G.; Morante, J.R. Synthesis and gas sensing properties of Pd-Doped SnO_2 nanocrystals. A case study of general morphology for doping metal oxides nanocrystals. *Cryst. Growth Des.* **2008**, *8*, 1774–1778.
31. Malyshev, V.V.; Pislyakov, A.V. Investigation of gas-sensitivity of sensor structures to hydrogen in a wide range of temperature, concentration and humidity of gas medium. *Sens. Actuators B Chem.* **2008**, *134*, 913–921.
32. Huang, Z.M.; Zhang, Y.Z.; Kotaki, M.; Ramakrishna, S. A review on polymer nanofibers by electrospinning and their applications in nanocomposites. *Compos. Sci. Technol.* **2003**, *63*, 2223–2253.
33. Wang, Z.; Liu, L. Synthesis and ethanol sensing properties of Fe-doped SnO_2 nanofibers. *Mater. Lett.* **2009**, *63*, 917–919.
34. Song, X.; Liu, L. Characterization of electrospun ZnO–SnO_2 nanofibers for ethanol sensor. *Sens. Actuators A* **2009**, *154*, 175–179.
35. Song, X.; Zhang, D.; Fan, M. A novel toluene sensor based on ZnO–SnO_2 nanofiber. *Appl. Surf. Sci.* **2009**, *255*, 7343–7347.
36. Park, J.A.; Moon, J.; Lee, S.J.; Lim, S.C.; Zyung, T. Fabrication and characterization of ZnO nanofibers by electrospinning. *Curr. Appl. Phys.* **2009**, *9*, S210–S212.
37. Liu, L.; Zhang, T.; Li, S.; Wang, L.; Tian, Y. Preparation, characterization, and gas-sensing properties of Pd-doped In_2O_3 nanofibers. *Mater. Lett.* **2009**, *63*, 1975–1977.
38. Zhang, H.; Li, Z.; Liu, L.; Wang, C.; Wei, Y.; MacDiarmid, G.A. Mg^{2+}/Na^{+}-doped rutile TiO_2 nanofiber mats for high-speed and anti-fogged humidity sensors. *Talanta.* **2009**, *79*, 953–958.
39. Wang, Y.; Ramos, I.; Santiago-Avilés, J.J. Detection of moisture and methanol gas using a single electrospun tin oxide nanofiber. *IEEE Sensors J.* **2007**, *7*, 1347–1348.

40. Lu, X.; Liu, X.; Zhang, W.; Wang, C.; Wei, Y. Large-scale synthesis of tungsten oxide nanofibers by electrospinning. *J. Colloid Interface Sci.* **2006**, *298*, 996–999.
41. Wang, G.; Ji, Y.; Huang, X.; Yang, X.; Gouma, P.I.; Dudley, M. Fabrication and characterization of polycrystalline WO_3 nanofibers and their application for ammonia sensing. *J. Phys. Chem. B* **2006**, *110*, 23777–23782.
42. Piperno, S.; Passacantando, M.; Santucci, S.; Lozzi, L.; La Rosa, S. WO_3 nanofibers for gas sensing applications. *J. Appl. Phys.* **2007**, *101*, 124504–124507.
43. Kudo, T.; Okamoto, H.; Matsumoto, K.; Sasaki, Y. Peroxopolytungstic acids synthesized by direct reaction of tungsten or tungsten carbide with hydrogen peroxide. *Inorg. Chim. Acta* **1986**, *111*, L27–L28.
44. Choi, S.-W.; Park, J.Y.; Kim, S.S. Dependence of gas sensing properties in ZnO nanofibers on size and crystallinity of nanograins. *J. Mater. Res.* **2011**, *26*, 1662–1665.
45. Choi, S.-W.; Park, J.Y.; Kim, S.S. Growth behavior and sensing properties of nanograins in CuO nanofibers. *Chem. Eng. J.* **2011**, *172*, 550–556.
46. Park, J.Y.; Asokan, K.M.; Choi, S.-W.; Kim, S.S. Growth kinetics of nanograins in SnO_2 fibers and size dependent sensing properties. *Sens. Actuators B Chem.* **2011**, *152*, 254–260.
47. Arbiol, J. Metal Additives Distribution in TiO_2 and SnO_2 Semiconductor Gas Sensor Nanostructured Materials. Ph.D. Thesis, Barcelona University, Barcelona, Spain, July 2001.